



# Plasma Electrolytic Oxidation of Arc-Sprayed Aluminum Coatings

Vasyl Pokhmurskii, Hrygorij Nykyforchyn, Mykhajlo Student, Mykhajlo Klappiv, Hanna Pokhmurska, Bernhard Wielage, Thomas Grund, and Andreas Wank

(Submitted March 12, 2007; in revised form June 10, 2007)

Different posttreatment methods, such as heat treatment, mechanical processing, sealing, etc., are known to be capable to improve microstructure and exploitation properties of thermal spray coatings. In this work, a plasma electrolytic oxidation of aluminum coatings obtained by arc spraying on aluminum and carbon steel substrates is carried out. Microstructure and properties of oxidized layers formed on sprayed coating as well as on bulk material are investigated. Oxidation is performed in electrolyte containing KOH and liquid glass under different process parameters. It is shown that thick uniform oxidized layers can be formed on arc-sprayed aluminum coatings as well as on solid material. Distribution of alloying elements and phase composition of obtained layers are investigated. A significant improvement of wear resistance of treated layers in two types of abrasive wear conditions is observed.

**Keywords** abrasive wear resistance, aluminum alloy, arc spray coating, microstructure, plasma electrolytic oxidation

## 1. Introduction

The method of plasma electrolytic oxidation (PEO), also called micro-arc oxidation (MAO), is very effective for production of protective and decorative coatings on aluminum profiles and other constructive elements. Its environmental friendliness is especially important for vehicles and constructions (aircrafts, boats, window frames, and siding of buildings). The method is used for treating of passivating class metals, such as aluminum, titanium, zirconium, etc., as well as their alloys. Aluminum parts coated with PEO layers show improved corrosion and wear resistance, increased breakdown voltage and

higher thermal stability. The big advantage of this technology is relative low cost. Numerous experimental results and discussion of tendencies in plasma electrolytic treatment for surface engineering are summarized in review (Ref 1). Some methods found an industrial implementation and are successfully used for a number of applications (Ref 2).

Further investigations are aimed on the optimization of process parameters in order to improve characteristics of PEO layers, minimization of residual stresses, increase of  $\alpha$ -Al<sub>2</sub>O<sub>3</sub> phase content and improvement of coating morphology (Ref 3). Results concerning modified PEO process ceramic coatings on 2024 series Al alloys that are suitable for tribological applications are reported in Ref 4. Corrosion, erosion, and erosion-corrosion performance of PEO deposits on 6082 alloy are studied in Ref 5. The effect of alloying of aluminum alloys by copper, magnesium, silicon, zinc, and lithium on the phase contents, thickness and microhardness of oxide-ceramic coatings were investigated in Ref 6.

Some new methods combining advantages of PEO layers and other surface treatment methods are recently developed. For example, the combination of micro plasma oxidation (MPO) and arc ion plating of TiN PVD coating represents a promising technique for surface modification of aluminum alloys for heavy surface load bearing application (Ref 7). Combined shot-peening and PEO treatment leads to increase of fatigue limit due to optimization of stress distribution and elevated microhardness compared to aluminum treated only with PEO (Ref 8).

The majority of investigations were carried out on bulk materials, and only few data are available that describe the results of PEO of coatings thermally sprayed on substrates made from materials that themselves cannot be oxidized, e.g., iron-based materials. Achievement of ceramic coatings with metallurgical bonding to steels using a combined method of arc spraying and PEO treatment is reported

This article is an invited paper selected from presentations at the 2007 International Thermal Spray Conference and has been expanded from the original presentation. It is simultaneously published in *Global Coating Solutions, Proceedings of the 2007 International Thermal Spray Conference*, Beijing, China, May 14-16, 2007, Basil R. Marple, Margaret M. Hyland, Yuk-Chiu Lau, Chang-Jiu Li, Rogerio S. Lima, and Ghislain Montavon, Ed., ASM International, Materials Park, OH, 2007.

Vasyl Pokhmurskii, Hrygorij Nykyforchyn, Mykhajlo Student, and Mykhajlo Klappiv, G.V. Karpenko Physico-Mechanical Institute of National Academy of Sciences of Ukraine, 5 a Naukova Str., 79603, Lviv, Ukraine; Hanna Pokhmurska, Bernhard Wielage, and Thomas Grund, Institute of Composite Materials, Chemnitz University of Technology, 09107, Chemnitz, Germany; and Andreas Wank, GTV Verschleiss-Schutz GmbH, 57629, Luckenbach, Germany. Contact e-mail: hanna.pokhmurska@mb.tu-chemnitz.de.

(Ref 9). However, to overcome poor adhesion of Al coatings to steel substrates a remelting of the coatings is carried out. That complicates the application of this method. Examples of aluminum thermal spray coating implementation with PEO layers for corrosion and wear protection of steel pump parts in chemical and petrol industry are presented in Ref 10. Finally, thermal protection of graphite-based composites can be provided by  $\text{Al}_2\text{O}_3$  layers formed on arc-sprayed aluminum coatings (Ref 11).

The results concerning microstructure, chemical composition, microhardness, and abrasive wear resistance of PEO layers formed on different substrates are presented in this article. A comparison of mentioned properties on aluminum surfaces and arc-sprayed aluminum coatings on aluminum alloy as well as on carbon steel substrates is given.

## 2. Experimental Procedure

### 2.1 Materials

Aluminum coatings are sprayed on specimens made from aluminum alloy D16 (Table 1) and carbon steel (Si:0.17-0.37, Mn:0.35-0.65, Cu:0.25, Ni:0.25, S:0.04, C:0.17-0.24, P:0.035, Cr:0.25, As:0.08).

AMh-6 aluminum alloy wires with the chemical composition given in Table 1 are arc-sprayed using with the following parameters: voltage: 32 V, current: 100 A, atomizing air pressure: 0.6 MPa, spraying distance: 100 mm. Coatings were formed using arc spraying equipment with the modernized spraying system (PhMI NANU) and differential dispersion scheme of electrode materials.

### 2.2 Oxidation Process

The oxide ceramic coatings are synthesized on aluminum substrate and on arc-sprayed aluminum coatings according to the scheme presented in Fig. 1 in the discharge channels of the metal-electrolyte system exposed to anode-cathode impulses of anodic current with a density of  $20 \text{ A/dm}^2$  and ratio of the cathodic and anodic current densities  $I_c/I_a$  equal to 1 and 1.5 during 90 and 120 min (Table 2).

This installation is described in detail in Ref 9 and consists of an electrical power supply and an electrolytic bath containing the specimen. Two different aqueous KOH electrolytes solutions with additions of sodium silicate are used (Table 2).

**Table 1** Chemical composition of used Al alloys (in wt.-%)

Alloy	Cu	Mg	Zn	Si	Mn	Fe
D16	3.8-3.9	1.2-1.8	0.8	0.4-0.5	0.3-0.9	0.4-0.5
AMh-6 <sup>a</sup>		5.8-6.8		0.4		0.4

<sup>a</sup>Zr: 0.2, Ti: 0.07-0.1

### 2.3 Coating Characterization

Coatings are characterized by metallographical investigation of coating cross sections. Optical microscope Olympus PME3 is applied for microstructure examinations and scanning electron microscope LEO 1455VP equipped with EDXS analyser Edison is used for estimation of the chemical composition. Vickers microhardness of coatings is measured under 100 g load. The phase composition of the coatings is determined by X-ray diffraction studies with  $\text{Cu } K\alpha$  radiation in the range  $2\theta$  between  $20^\circ$  and  $120^\circ$  using Siemens D5000 equipment.

Resistance against wear by bound abrasive is determined in corundum grinding disk test. Also resistance against abrasive wear by loose particles is tested according to ASTM G65. Wear is determined gravimetrically by weighing. According to ASTM G65 test, quartz sand dried to a moisture content of  $\leq 0.16\%$  is delivered into the zone of friction of a rubber disk against the surface of the specimen. The diameter of the disk was equal to 50 mm, its width to 15 mm, and the frequency of rotation to  $2.1 \text{ s}^{-1}$  (25 m/min). The disk was pressed to the specimen by a force  $P = (44.1 \pm 0.25) \text{ N}$  during 300 s. In the process of friction of specimens against a rigidly fixed abrasive, we used an abrasive wheel 150 mm in diameter and 8 mm in width

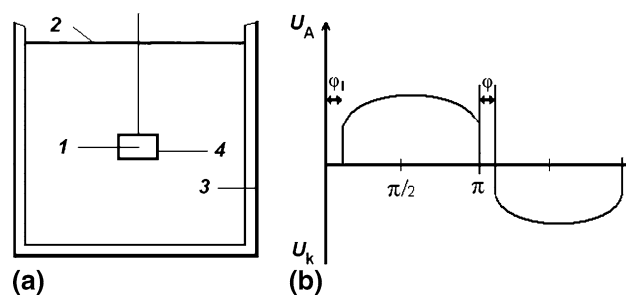


**Fig. 1** Principle scheme of oxidation process (a) general application; (b) voltage-time function; 1: working electrode; 2: electrolyte; 3: bath; 4: discharge channel

**Table 2** Processing conditions of the investigated coatings

Material	Electrolyte	Anodic current $I_a$ , $\text{kA/m}^2$	Cathodic current $I_c$ , $\text{kA/m}^2$	Duration, min
1-0	D16	1	2	120
1	D16+TS Al	1	2	120
2-0	D16	1	2	120
2	D16+TS Al	1	2	120
3	Steel+TS Al	1	2	120
4	Steel+TS Al	1	2	120
5-0	D16	2	2	90
5	D16+TS Al	2	2	90
6-0	D16	2	2	120
6	D16+TS Al	2	2	120
7	Steel+TS Al	2	2	120

1: 3 g/L KOH + 2 g/L sodium silicate  $\text{Na}_2\text{SiO}_4$

2: 10 g/L KOH + 15 g/L sodium silicate  $\text{Na}_2\text{SiO}_4$  + 0.1 g/L  $\text{CrO}_2$

made of SM-2-type corundum with grains 20  $\mu\text{m}$  in size. The frequency of rotation was equal to  $2.7 \text{ s}^{-1}$  (58 m/min). The load in the zone of linear contact  $P = (14.7 \pm 0.25) \text{ N}$  was applied during 1800 s. The degree of wear was measured as the loss of mass of the specimens with an accuracy of 100  $\mu\text{g}$ .

### 3. Results and Discussion

#### 3.1 Arc-Sprayed Coatings Microstructure

Applied modified arc spray torch provides a decreasing of size and an increasing of velocity of spraying particles that result in the formation of very dense and homogeneous aluminum coatings (Fig. 2). Porosity of sprayed coatings is lower than 3-4%. Adhesion of aluminum coatings sprayed on aluminum alloy substrate is 10-12 MPa and for spraying on steel substrates not lower than 20 MPa. Thickness of sprayed coatings is varied in a range from 150 to 1.5 mm. Microhardness of arc-sprayed coatings is 90-95 HV0.1.

#### 3.2 Kinetic of PEO Coating Growth on Solid Substrate

As it has been shown earlier for oxidation of solid substrates (Ref 9, 12), the anode-cathode method of oxide ceramics formation allows to decrease the porosity of oxide layer and thus to obtain coatings with higher density and 1.3-1.5 times higher microhardness than for PEO coatings obtained on the D16 substrate by direct current method. By increasing the synthesis time it is possible to form coatings with the thickness up to 500  $\mu\text{m}$ .

The time dependence of coating thickness growth is determined by process parameters. This dependence is shown in Fig. 3 and can be divided in four stages. The first one (few minutes of synthesis) corresponds to the formation of a primary oxide film. The homogeneous growth of the oxide ceramic coating takes place at the second and third stages (with different rates).

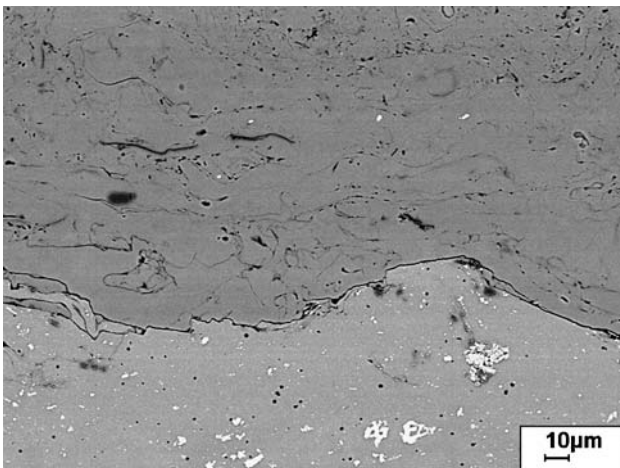


**Fig. 2** SEM micrograph of an arc-sprayed AMh-6 coating on D16 aluminum substrate

For stages II and III a coating growth rate is about 2  $\mu\text{m}/\text{min}$  for thickness between 50 and 100  $\mu\text{m}$  and about 1  $\mu\text{m}/\text{min}$  in the thickness range between 100 and 400  $\mu\text{m}$ , respectively. At the last stage of the conversion process the thickness rate decreases nonlinearly. Under the present formation conditions coatings with thickness exceeding 500  $\mu\text{m}$  can undergo cracking.

#### 3.3 Microstructure of PEO Coatings

Typical micrographs of polished sections of coatings produced by the PEO technique on an aluminum alloy and on an arc-sprayed coating, obtained using scanning electron microscopy, are shown in Fig. 4a and b, respectively. PEO coatings formed on all investigated substrates show a typical microstructure with some distinct regions, i.e., porous top region, intermediate region with low porosity and a thin interfacial region near the interface with the aluminum substrate or aluminum coating. Intermediate layers seem to be practically pores free, but the big magnification proves the evidence of a network of fine, surface-connected pores. According to the image analysis of such sections that has been carried out by several authors (i.e., Ref 13) one can estimate that typical porosity levels for such structure are below 3%.

The relative dimensions of these regions, their structure, and composition strongly depend on treatment parameters as well as on substrate and electrolyte composition. Oxide coatings produced on aluminum substrates in more concentrated solution have much more extended outer, so called technological, layers that can reach up to 80-90% of general coating thickness and generally are rather porous (Fig. 5).

PEO coatings formed on aluminum coatings sprayed on steel substrates under all applied parameters demonstrate uniform microstructure with very good adhesion of

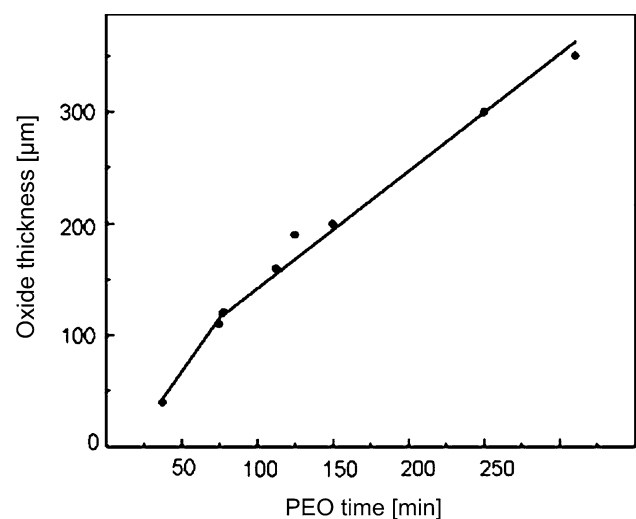


**Fig. 3** Kinetics of the coating growth on D16 alloy at current density:  $2 \text{ kA}/\text{m}^2$ ,  $I_c/I_a$  0.9, electrolyte: 0.1% KOH + 0.1% water glass

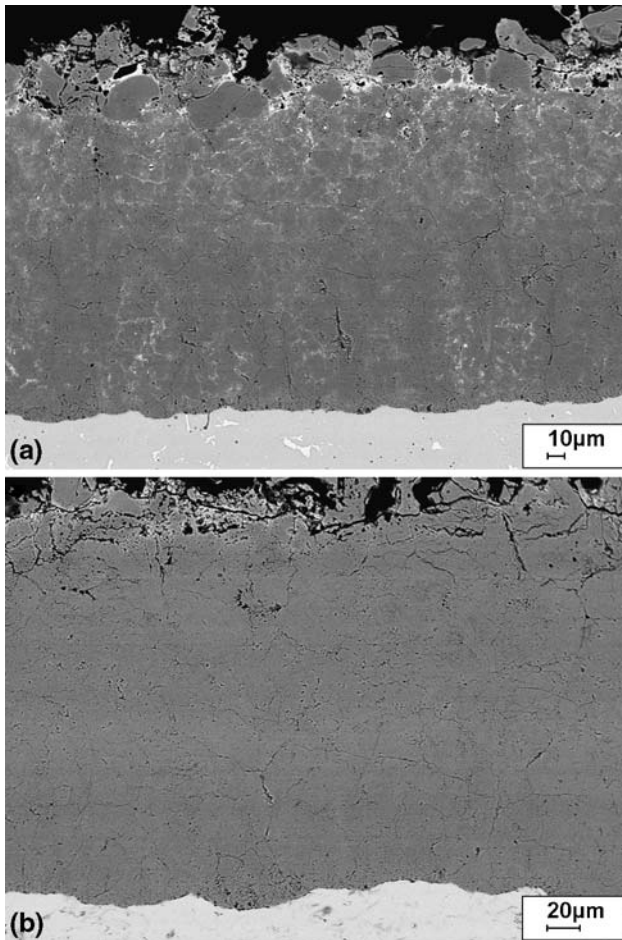
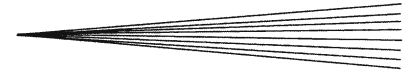


**Fig. 4** SEM micrographs of oxide coatings produced by the PEO technique on an aluminum alloy (a) and on an arc-sprayed coating (b) at current density  $2 \text{ kA/m}^2$ ,  $I_c/I_a$  1.0 in electrolyte 1

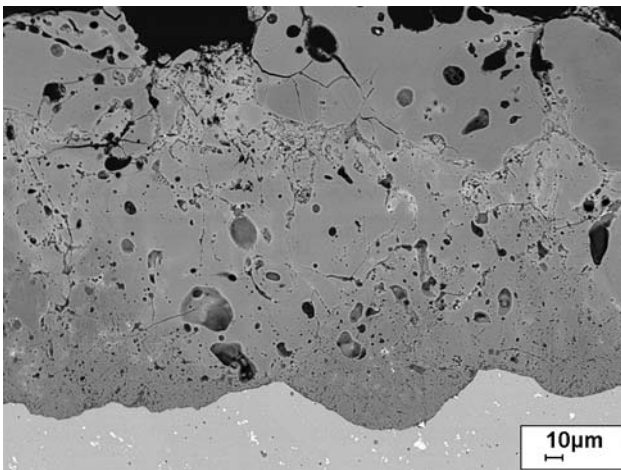


**Fig. 5** SEM micrograph of an oxide coating produced by the PEO technique on aluminum alloy D16 at current density  $2 \text{ kA/m}^2$ ,  $I_c/I_a$  1.0 in electrolyte 2 within 90 min

PEO layers to coatings. The increase of  $I_c/I_a$  ratio from 1.0 to 1.5 as well as application of more concentrated electrolytic solution leads to formation of coatings with smaller roughness and thinner porous technological region on top (Fig. 6).

### 3.4 Elemental Distribution

Chemical composition of oxidized layers depends on the substrate material, but generally the character of element distribution in PEO coatings formed on solid aluminum and on the arc-sprayed coatings are similar (Tables 3 and 4). The slightly higher content of Mg in PEO layers formed on arc-sprayed coatings and the appearance of copper in PEO coatings formed on D16 occurs due to the difference in chemical composition of solid material and coating. In both coatings the concentration of alloying elements (e.g., Cu and Mg) increases toward the surface. Chemical composition of PEO coatings formed on the arc-sprayed aluminum coatings does not depend on the type of applied substrate.

In the photo of Fig. 4a, Cu distribution in the PEO layer formed on bulk aluminum alloy D16 is clearly visible (white appeared areas). Such element segregation can be explained by selective element evaporation in melted channel due to the different partial vapor pressure values. In the near surface areas of the oxidized layers small amounts of Si, Na, Ca, and K are detected by EDX analysis.

### 3.5 Phase Analysis

X-ray analyses of PEO coatings show some part of amorphous phase that is present in oxidized layers. Coatings consist of different shares of  $\alpha$ - and  $\gamma(\sigma)$ -phase alumina. The ratio  $\alpha/(\gamma + \sigma)$  depends on the alloy composition and anodising process parameters. Coatings that are produced on solid aluminum in accordance with the parameter set 2 show the highest content of  $\alpha\text{-Al}_2\text{O}_3$ , i.e., 73%. Coatings produced on arc spray coatings under the same conditions contain 18% of  $\alpha\text{-Al}_2\text{O}_3$  and 82% of  $(\gamma + \sigma)$ -phase. Phase composition of PEO layers depends strongly on cooling rates of melt areas in spark channels. For solid aluminum alloy they are lower comparing to that in thermal-sprayed coatings due to the porosity, which is a reason of saturating of coating with electrolyte solution and in that way the porosity insures the higher cooling rates. As a result a higher percentage of  $\gamma$ - (and  $\sigma\text{-Al}_2\text{O}_3$  phases is formed. Treatment in more concentrated electrolytic solution also leads to decrease of  $\alpha\text{-Al}_2\text{O}_3$  content, e.g., to 7% for PEO layers obtained in accordance with parameter set 7.

### 3.6 Microhardness of PEO Coatings

Microhardness of PEO coatings depends on processing parameters as well as on the material of substrate. In Fig. 7 distributions of microhardness values in PEO coating obtained in bulk aluminum alloy D16 (curves 1-0, 2-0) and in arc-sprayed Al coatings (curves 1, 2) measured on cross sections in the direction from surface to substrate are presented.

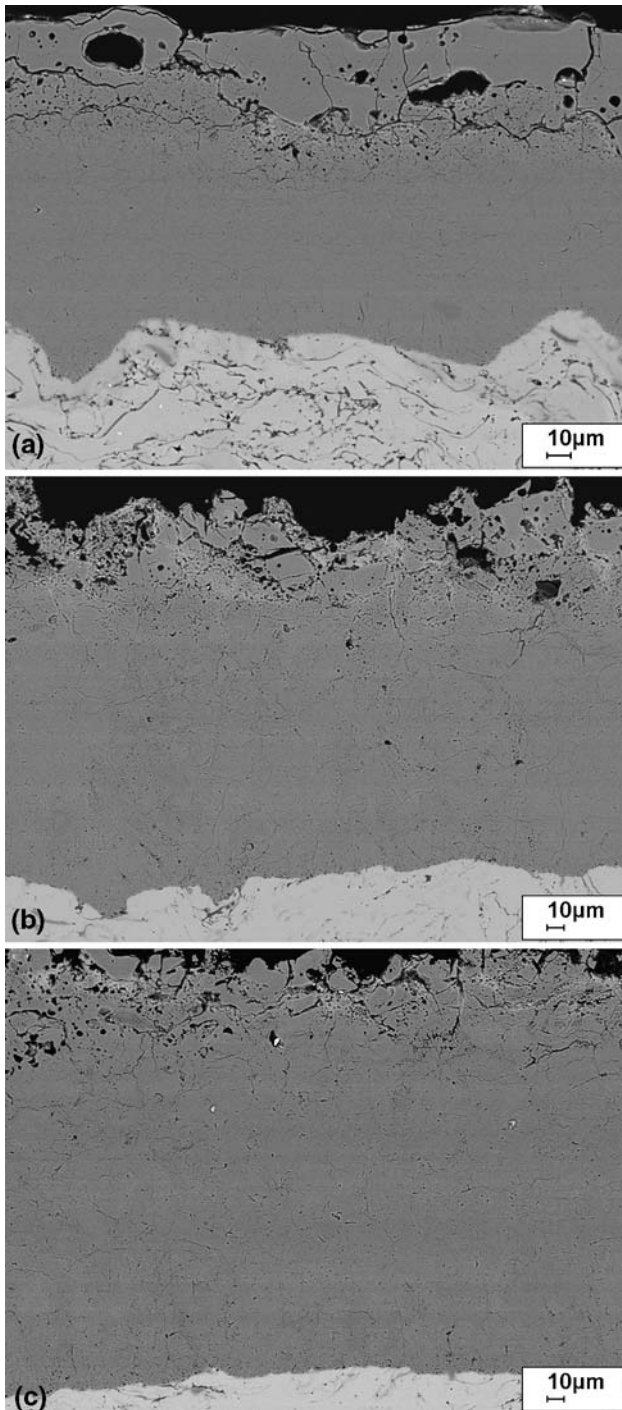


**Fig. 6** SEM micrographs of oxide coatings produced by the PEO technique on arc sprayed aluminum coatings at current density  $2 \text{ kA/m}^2$ ,  $I_c/I_a$  1.0 in electrolyte 1 (a),  $I_c/I_a$  1.5 in electrolyte 1 (b), and  $I_c/I_a$  1.0 in electrolyte 2 (c)

The highest microhardness, i.e., 1800-2000 HV0.1 is achieved for oxidized layers on solid material due to the higher content of  $\alpha\text{-Al}_2\text{O}_3$  (Fig. 7). PEO coatings formed on arc-sprayed coatings show values 10-15% lower, i.e., 1600-1700 HV0.1. Increase of the cathodic/anodic current

**Table 3** EDS analyses of PEO layers formed on arc-sprayed Al coatings

	Initial coating		PEO layer					
			Average		Center		Top	
	at.%	wt.%	at.%	wt.%	at.%	wt.%	at.%	wt.%
Na	...	...	0.1	0.1	...	...	0.1	0.1
Mg	4.4	4.1	1.5	1.8	1.0	1.2	1.6	1.9
Al	90.2	92.5	41.1	50.5	38.3	51.0	37.2	49.3
Si	0.3	0.3	0.2	0.3	0.2	0.2	0.9	1.3
K	...	...	...	...	...	...	0.3	0.5
O	5.2	3.1	60.1	47.3	60.5	47.6	59.9	46.9

**Table 4** EDS analyses of PEO layers formed on solid D16

	Alloy		PEO layer					
			Average		Center		Top	
	at.%	wt.%	at.%	wt.%	at.%	wt.%	at.%	wt.%
Na	...	...	0.3	0.3	...	...	0.3	0.3
Mg	1.7	1.6	0.8	0.9	0.4	0.4	0.9	1.0
Al	94.6	93.8	37.6	48.8	37.4	49.5	32.9	42.6
Si	0.3	0.3	0.8	1.1	0.5	0.7	3.2	4.2
K	...	...	0.2	0.5	0.1	0.3	1.1	2.2
Ca	...	...	...	...	...	...	0.1	0.3
Cu	1.4	3.2	0.9	2.7	0.3	1.0	1.0	3.0
O	2.0	1.1	59.5	45.7	61.3	48.1	60.5	46.4

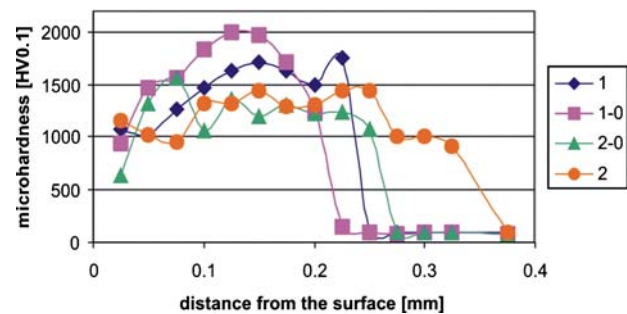


**Fig. 7** Distribution of microhardness in PEO coatings on solid aluminum alloy D16 (1-0, 2-0) and on arc-sprayed aluminum coating (1, 2); process parameters according to Table 2

ratio from  $I_c/I_a = 1.0$ -1.5 leads to decreased microhardness of both PEO layers on solid material and arc-sprayed coatings, i.e., 1350-1550 HV0.1 and 1300-1450 HV0.1, respectively. There is no significant difference for coatings sprayed on aluminum or steel substrates.

### 3.7 Wear Behavior

Wear resistance of PEO layers is determined in two wear tests: resistance against wear by bound abrasive by corundum grinding disk test and against abrasive wear by loose particles according to ASTM G65. The average data for both tests are shown in Fig. 8a and b, respectively. For comparison aluminum alloy D16 and low-alloyed

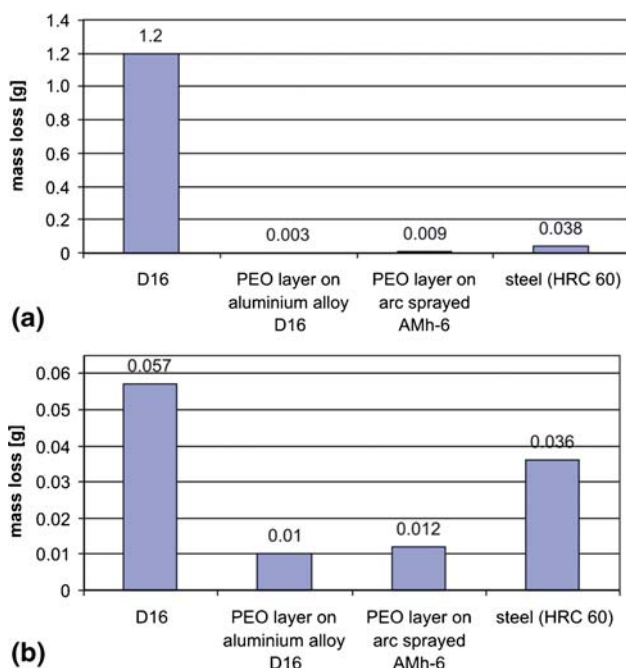


**Fig. 8** Results of corundum grinding disk wear test (a; test conditions: load—1.5 kg, duration—30 min) and ASTM G65 (b) wear test

high-speed steel with HRC 60 are tested. Like in corundum grinding disk tests, PEO layers obtained on the solid aluminum alloy show strong advantages concerning wear resistance in ASTM G65 tests in comparison to the untreated aluminum alloy and the high-speed steel. Higher wear resistance of PEO layers on solid aluminum alloys can be explained by the higher content of  $\alpha$ - $\text{Al}_2\text{O}_3$  phase in the respective coatings. Table 5 summarizes some relative data concerning wear resistance of different thermal-sprayed coating materials obtained in corundum grinding disk investigations. As a reference material a bulk D16 aluminum alloy is considered. PEO coatings show better wear resistance than the larger variety of materials that are commonly used for wear protection coatings in different applications.

#### 4. Summary and Conclusions

Plasma electrolytic oxidation of aluminum coatings obtained by arc spraying on aluminum and steel substrates in comparison to PEO coatings on solid aluminum alloy is carried out. It is shown that coating microstructure, phase and chemical composition depend on processing parameters. The highest content of  $\alpha$ - $\text{Al}_2\text{O}_3$  phase that provides the highest microhardness of up to 2000 HV0.1 in the oxidized layer is observed for PEO layers produced directly on the solid aluminum alloy. PEO layers obtained on arc-sprayed aluminum coatings have lower content of  $\alpha$ - $\text{Al}_2\text{O}_3$  phase and thus microhardness is decreased to a maximum of 1500 HV0.1. A significant improvement of

**Table 5** Comparative results of corundum grinding disk wear test for different materials<sup>a</sup>

Tested material	Relevant wear resistance
Aluminum alloy D16 (reference material)	1
Low-alloyed high-speed steel HRC 60	30
Hardened steel HRC 62	50
Arc-sprayed cored wire (60% FeCrB, 40% Al)	60
Arc-sprayed cored wire (55% SiC, 45% NiBSi)	90
Arc-sprayed cored wire (55% TiO <sub>2</sub> , 45% NiBSi)	100
PEO layer on arc-sprayed AMh-6	130
Laser dispersion of SiC in Al alloy 7075	200
VPS iron-based hard alloy coating (high VC content)	240
PEO layer on aluminum alloy D16	400

<sup>a</sup>All data obtained by authors in previous investigations

wear resistance of PEO layers under two types of wear conditions is observed. Wear resistance of PEO coatings obtained on arc-sprayed aluminum coatings is slightly worse than for layers obtained on solid material, but higher than for many industrially applied wear protection coatings. The obtained results show that plasma electrolytic oxidation of thermal-sprayed aluminum coatings is a promising route for protection of steel components against wear and/or corrosion.

#### References

1. A.L. Yerokhin, X. Nie, A. Leyland, A. Matthews, and S.J. Dowey, Plasma Electrolysis for Surface Engineering, Review, *Surf. Coat. Technol.*, 1999, **122**, p 73-93
2. V.V. Bakovec, O.V. Polakov, and I.P. Dolgovsova, Plasma Electrolytic Anodic Treatment of Metals. Publishing House, Nauka, Novosibirsk, 1990
3. A. Wilde, Ceramic-Base Surface Treatment Technology for Light-Metal Alloys, *Ind. Heat.*, 2005, **72**(2), p 61-65
4. S. Shrestha, A. Sturgeon, P. Shashkov, and A. Shatrov, Improved Corrosion Performance of AZ91D Magnesium Alloy Coated with the Keronite Process, *Proc. Magnesium Technology Symp.*, 2002, TMS Annual Meeting, 2002, Vol. 131, p 283-287
5. R.H.U. Khan, A.L. Yerokhin, T. Pilkington, A. Leyland, and A. Matthews, Residual Stresses in Plasma Electrolytic Oxidation Coatings on Al Alloy Produced by Pulsed Unipolar Current, *Surf. Coat. Technol.*, 2005, **200**(5-6), p 1580-1586
6. A.L. Yerokhin, A. Shatrov, V. Samsonov, P. Shashkov, A. Pilkington, A. Leyland, and A. Matthews, Oxide Ceramic Coatings on Aluminium Alloys Produced by a Pulsed Bipolar Plasma Electrolytic Oxidation Process, *Surf. Coat. Technol.*, 2005, **199**(2-3), p 150-157
7. R.C. Barik, J.A. Wharton, R.J.K. Wood, K.R. Stokes, and R.L. Jones, Corrosion, Erosion and Erosion-Corrosion Performance of Plasma Electrolytic Oxidation (PEO) Deposited Al<sub>2</sub>O<sub>3</sub> Coatings, *Surf. Coat. Technol.*, 2005, **199**(2-3), p 158-167
8. X. Nie, E.I. Meletis, J.C. Jiang, A. Leyland, A.L. Yerokhin, and A. Matthews, Abrasive Wear/Corrosion Properties and TEM Analysis of Al<sub>2</sub>O<sub>3</sub> Coatings Fabricated Using Plasma Electrolysis, *Surf. Coat. Technol.*, 2002, **149**(2-3), p 245-251
9. H.M. Nykyforchyn, M.D. Klapkiv, and V.M. Posuvailo, Properties of Synthesised Oxide-Ceramic Coatings in Electrolyte Plasma on Aluminium Alloys, *Surf. Coat. Technol.*, 1998, **100-101**, p 219-221
10. H. Awad-Samir and H.C. Qian, Deposition of Duplex Al<sub>2</sub>O<sub>3</sub>/TiN Coatings on Aluminum Alloys for Tribological Applications

- Using a Combined Microplasma Oxidation (MPO) and Arc Ion Plating (AIP), *Wear*, 2005, **260**(1-2), p 215-222
11. D.T. Asquith, A.L. Yerokhin, J.R. Yates, and A. Matthews, Effect of Combined Shot-Peening and PEO Treatment on Fatigue Life of 2024 Al Alloy, *Thin Solid Films*, 2006, **515**(3), p 1187-1191
  12. I.P. Mertsalo, V.T. Yavorskii, M.D. Klaviv, and R.S. Mardarevych, Wear Resistance of Anodic-Spark Coatings on Aluminium Alloy, *Mater. Sci.*, 2003, **39**(1), p 136-139
  13. A. Curran and T.W. Clyne, Porosity in Plasma Electrolytic Oxide Coatings, *Acta Materialia*, 2006, **54**, p 1985-1993